Molecular Pharmacology Fast Forward. Published on October 3, 2018 as DOI: 10.1124/mol.118.113142
This article has not been copyedited and formatted. The final version may differ from this version.

Title Page

Activated CaMKIIα binds to the mGlu$_5$ metabotropic glutamate receptor and modulates calcium mobilization

Christian R. Marks, Brian C. Shonesy, Xiaohan Wang, Jason R. Stephenson, Colleen Niswender, Roger J. Colbran

Department of Molecular Physiology and Biophysics (C.R.M., B.C.S., J.R.S., R.J.C.), Vanderbilt Brain Institute (X.W., R.J.C.), Vanderbilt Kennedy Center for Research on Human Development (C.N., R.J.C.), Department of Pharmacology (C.N.), Vanderbilt Center for Neuroscience Drug Discovery (C.N.), Vanderbilt University School of Medicine, Nashville, TN, USA

Molecular Pharmacology Fast Forward. Published on October 3, 2018 as DOI: 10.1124/mol.118.113142
This article has not been copyedited and formatted. The final version may differ from this version.

Running Title Page

Running title: CaMKII modulates $mGlu_5$ by interaction with the CTD

Correspondence address: Roger J. Colbran, Ph.D., Room 702 Light Hall, Vanderbilt University School of Medicine, Nashville, TN 37232-0615. Tel.: 615-936-1630; Fax: 615-322-7236; E-mail: roger.colbran@vanderbilt.edu.

Text Pages: 40

Number of figures: 7

Number of references: 64

Number of words in Abstract: 207

Number of words in Introduction: 659

Number of words in Discussion: 1,384

Abbreviations: CaMKII, Calcium Calmodulin Dependent Protein Kinase II; CA-CaMKII, constitutively active CaMKII; CaM, Calmodulin; CaMKAP, CaMKII Associated Protein; CTD, C-terminal Domain; D_2R, D2 Dopamine Receptor; D_3R, D3 Dopamine Receptor; GPCR, G protein-coupled receptor, GST, Glutathione S-Transferase, GST-$mGlu_{5a}$-CTD, GST tagged $mGlu_{5a}$ construct containing residues 827-964; KO, knock-out; LTD, long term depression; LTP, long term potentiation; mGlu, metabotropic glutamate receptor; $mGlu_1$, metabotropic glutamate receptor 1; $mGlu_5$, metabotropic glutamate receptor 5; PKA, protein kinase A; PKC, protein kinase C; WT, wild-type.

Molecular Pharmacology Fast Forward. Published on October 3, 2018 as DOI: 10.1124/mol.118.113142
This article has not been copyedited and formatted. The final version may differ from this version.

Abstract

Ca^{2+} calmodulin dependent protein kinase II (CaMKII) and metabotropic glutamate receptor 5 ($mGlu_5$) are critical signaling molecules in synaptic plasticity and learning memory. Here, we demonstrate that $mGlu_5$ is present in CaMKIIα complexes isolated from mouse forebrain. Further *in vitro* characterization showed that the membrane-proximal region of the C-terminal domain (CTD) of $mGlu_{5a}$ directly interacts with purified Thr286-autophosphorylated (activated) CaMKIIα. However, the binding of CaMKIIα to this CTD fragment is reduced by the addition of excess Ca^{2+}/calmodulin or by additional CaMKIIα autophosphorylation at non-Thr286 sites. Furthermore, *in vitro* binding of CaMKIIα is dependent on a tribasic residue motif Lys-Arg-Arg (KRR) at residues 866-868 of the $mGlu_{5a}$-CTD, and mutation of this motif decreases the co-immunoprecipitation of CaMKIIα with full-length $mGlu_{5a}$ expressed in heterologous cells by about 50%. The KRR motif is required for two novel functional effects of co-expressing constitutively active CaMKIIα with $mGlu_{5a}$ in heterologous cells. First, cell-surface biotinylation studies showed that CaMKIIα increases the surface-expression of $mGlu_{5a}$. Second, using Ca^{2+} fluorimetry and single-cell Ca^{2+}-imaging, we found that CaMKIIα reduces the initial peak of $mGlu_{5a}$-mediated Ca^{2+} mobilization by about 25%, while doubling the relative duration of the Ca^{2+} signal. These findings provide new insights into the physical and functional coupling of these key regulators of postsynaptic signaling.

Molecular Pharmacology Fast Forward. Published on October 3, 2018 as DOI: 10.1124/mol.118.113142
This article has not been copyedited and formatted. The final version may differ from this version.

Introduction

The ability of excitatory glutamatergic synapses to undergo dynamic changes in strength, termed synaptic plasticity, is critical for many behaviors. It is well established that glutamate activation of diverse ionotropic and metabotropic receptors is critical for short- and long-term control of many neuronal responses (Niswender and Conn, 2010), and that these responses require a complex and incompletely understood network of signaling proteins. Among the 7 members of the metabotropic glutamate (mGlu) receptor family, $mGlu_1$ and $mGlu_5$ specifically couple through $G\alpha_{q/11}$ to stimulate multiple signaling pathways, including phosphoinositide hydrolysis and mobilization of intracellular Ca^{2+} stores. These receptors have long been implicated in multiple forms of long-term depression (LTD) that require new protein synthesis (Huber et al., 2001; Oliet et al., 1997; Palmer et al., 1997) or increased endocannabinoid signaling (Luscher and Huber, 2010). Despite many similarities, $mGlu_1$ and $mGlu_5$ can be differentially regulated by various mechanisms and have been shown to have different neuronal roles. For instance, in hippocampus, $mGlu_1$ increases the frequency of spontaneous inhibitory post synaptic currents while $mGlu_5$ potentiates NMDA receptor currents (Mannaioni et al., 2001). In particular, $mGlu_5$ has been specifically implicated in a number of neuropsychiatric disorders including addiction, schizophrenia, Fragile X Syndrome, Obsessive Compulsive Disorder, and Alzheimer's Disease (Ade et al., 2016; Foster and Conn, 2017; Grueter et al., 2008; Hu et al., 2014; Michalon et al., 2012; Ronesi et al., 2012).

Like $mGlu_5$, Ca^{2+}/calmodulin (CaM)-dependent protein kinase II α (CaMKIIα) is a key signaling protein in dendritic spines. CaMKIIα is activated by Ca^{2+}/CaM binding and undergoes autophosphorylation at Thr286 (Baucum et al., 2015; Miller et al., 1988; Mukherji et al., 1994; Rich and Schulman, 1998; Yang and Schulman, 1999). Thr286 autophosphorylation increases

Molecular Pharmacology Fast Forward. Published on October 3, 2018 as DOI: 10.1124/mol.118.113142
This article has not been copyedited and formatted. The final version may differ from this version.

the affinity for Ca^{2+}/CaM and stabilizes the kinase in a constitutively active conformation. This constitutive activity is essential for normal synaptic plasticity in many brain regions (Coultrap et al., 2014; Giese et al., 1998; Jin et al., 2015; Mockett et al., 2011; Shonesy et al., 2014; Silva et al., 1992a; Silva et al., 1992b; Zhou et al., 2007) including $mGlu_{1/5}$-dependent long term depression (LTD) in the hippocampus (Huber et al., 2001; Mockett et al., 2011). Interestingly, both CaMKIIα- and $mGlu_5$-knockout mice display deficits in learning and memory and hippocampal synaptic plasticity (Huber et al., 2001; Jia et al., 1998; Simonyi et al., 2005). Although both $mGlu_5$ and CaMKII are critical to many forms of plasticity, a functional link between the two has not been widely investigated.

The intracellular C-terminal domains (CTDs) of $mGlu_1$ and $mGlu_5$ have emerged as important loci for regulation by protein binding and phosphorylation (Enz, 2012; Mao and Wang, 2016). While there are two splice variants of $mGlu_5$ ($mGlu_{5a}$ and $mGlu_{5b}$), most studies have focused on $mGlu_{5a}$ and few pharmacological differences between splice variants have been identified (Joly et al., 1995; Minakami et al., 1995; Romano et al., 1996). The $mGlu_5$-CTD has been shown to bind to a number of different proteins including Ca^{2+}/CaM and Homer to regulate cell surface expression of the receptor (Choi et al., 2011; Lee et al., 2008; Roche et al., 1999; Saito et al., 2002). Protein kinase A (PKA) and protein kinase C (PKC) also regulate $mGlu_5$ surface expression through phosphorylation of the CTD (Mao et al., 2008; Uematsu et al., 2015). It was recently reported that CaMKII can bind to the CTD and intracellular loop 2 of both $mGlu_1$ and $mGlu_5$ (Jin et al., 2013b; Raka et al., 2015) and that CaMKII modulates $mGlu_5$ agonist-induced internalization and ERK1/2 activation (Raka et al., 2015). Here, we identify three basic residues (Lys^{866}-Arg^{877}-Arg^{888}) in the membrane proximal region of the $mGlu_{5a}$-CTD that are essential for a direct interaction with activated CaMKIIα, and provide novel insights into multiple factors that

Molecular Pharmacology Fast Forward. Published on October 3, 2018 as DOI: 10.1124/mol.118.113142
This article has not been copyedited and formatted. The final version may differ from this version.

modulate the interaction. We also show that CaMKII binding to the CTD is important for the regulation of $mGlu_5$ surface expression and Ca^{2+} mobilization. These data provide novel insights into the molecular basis and function of the $mGlu_5$-CaMKII interaction that may be involved in synaptic plasticity.

Materials and methods

DNA constructs

The GST-$mGlu_{5a}$-CTD expression construct was created by PCR amplification of the region encoding residues 827-964 of $mGlu_{5a}$ (NP_058708.1) using primers 5'CTGGAAGTTCTGTTCCAGGGGCCCGGATCCAAACCGGAGAGAAAT 3' (Forward) and 5' GCCGCAAGCTTGTCGACGGAGCTCGAATTCTTAGGTCCCAAAGCGCTT 3' (Reverse) and inserting the product into BamHI/EcoR1 sites of pGEX6P using a sequence and ligation independent cloning (SLIC) cloning protocol (Li and Elledge, 2012).

The pCGN plasmid to express WT $mGlu_{5a}$ with an N-terminal HA-tag was made by amplifying the entire rat $mGlu_{5a}$ coding sequence (forward primer: 5'TGACGTGCCTGACTATGCCTCTAGAATGGTCCTTCTGTTGATCCT3'; reverse primer: 5' ACTCACCCTGAAGTTCTCAGGATCCTCACAACGATGAAGAACTCT3') and inserting the fragment into XbaI and BamHI restriction sites of the empty pCGN plasmid (a gift from Dr. Winship Herr, Université de Lausanne, Switzerland, Addgene plasmid ID 53308).

The $K^{866}RR^{868}$ mutation to AAA in $mGlu_{5a}$ was generated by site-directed mutagenesis of the pGEX6P or pCGN constructs (see above) using a Quick Change protocol (Agilent) with the following primers

5'GGGTTTCCCCAGAGGAGC**CGGCGGCGG**CCCACAGGTTGACTAGGCTGCT3'

Molecular Pharmacology Fast Forward. Published on October 3, 2018 as DOI: 10.1124/mol.118.113142
This article has not been copyedited and formatted. The final version may differ from this version.

(Forward) and

5'AGCAGCCTAGTCAACCTGTGGG**CCGCCGCCGG**CTCCTCTGGGGAAACCC3'

(Reverse).

We used pcDNA3.1 constructs to express untagged and mApple-tagged WT-CaMKIIα and a constitutively active T286D/T305A/T306A triple mutant of CaMKIIα (CA-CaMKIIα), as previously described (Jalan-Sakrikar et al., 2012; Jiao et al., 2008; Stephenson et al., 2017). In the CA-CaMKIIα, the phospho-mimetic T286D mutation results in constitutive CaMKIIα activity and the phospho-null T305A/T306A mutations prevent CaMKIIα phosphorylation at these sites, which interferes with binding of Ca^{2+}/CaM and α-actinin (Jalan-Sakrikar et al., 2012).

Recombinant protein purification

Expression and purification of recombinant mouse CaMKIIα has been described before (McNeill and Colbran, 1995). To express GST-tagged proteins, pGEX6P-1 plasmids were transformed into BL21(DE3) bacteria cells. Cells were grown in LB media at 37°C to reach OD~0.6. Cells were cooled to room temperature and IPTG (0.2 mM) was then added to induce protein expression for 12-16 hours. Inducing protein expression at room temperature substantially reduced protein degradation seen when proteins were expressed at 37°C. Expressed proteins were purified using Pierce Glutathione Agarose beads (Cat. #16101) following manufacture's instruction. Eluted proteins were then dialyzed in 10 mM HEPES pH 7.5, 25 μM PMSF, 62.5 μM Benzamidine, 62.5 μM EDTA, 0.1% Triton X-100 overnight with one buffer change.

CaMKIIα autophosphorylation

Molecular Pharmacology Fast Forward. Published on October 3, 2018 as DOI: 10.1124/mol.118.113142
This article has not been copyedited and formatted. The final version may differ from this version.

Purified mouse CaMKIIα was autophosphorylated under two different conditions. Typically, CaMKIIα was incubated with 50 mM HEPES, pH 7.5, 10 mM $Mg(CH_3\text{-}COO)_2$, 0.5 mM $CaCl_2$, 2 μM CaM, 40 μM ATP on ice for 90 s before addition of EDTA and EGTA (20 mM final) to terminate phosphorylation by chelation of Mg^{2+} and Ca^{2+}. Similar conditions were previously shown to result in the selectively autophosphorylation of Thr286 (McNeill and Colbran, 1995). Where indicated, identical autophosphorylation reactions were incubated for 10 minutes at 30°C to perform a more extensive phosphorylation at several additional sites (Baucum et al., 2015).

GST pulldown and CaM binding competition

Purified GST-mGlu$_5$-CTD (1 μM) and CaMKIIα (62.5 nM; pre-autophosphorylated as indicated in figure legends) were incubated at 4°C in GST-pulldown buffer (50 mM Tris-HCl pH 7.5; 150 mM NaCl; 1% (v/v) Triton X-100) with either 2 mM EGTA or 2.5 mM $CaCl_2$ plus 10 μM calmodulin, as indicated. An aliquot (5%) of each incubation was saved as an input sample. After 1 h, pre-washed glutathione agarose beads (Pierce Cat. #16101) (15 μl of a 50:50 slurry) were added and incubation was continued at 4°C for an additional 1 h. The beads were then separated by centrifugation (2000 x g, 30 s), and washed three times with GST-pulldown buffer containing either 2 mM EGTA or 2.5 mM $CaCl_2$, respectively. Beads were then incubated at 4°C with GST pulldown buffer containing 20 mM glutathione, adjusted to pH 8.0, for 10 min. After centrifugation, eluted proteins were transferred to a new tube, mixed with 4X SDS-PAGE buffer and heated for 10 minutes at 90°C prior to SDS-PAGE and Western Blot analysis.

Cell culture, transfection and immunoprecipitation

Molecular Pharmacology Fast Forward. Published on October 3, 2018 as DOI: 10.1124/mol.118.113142
This article has not been copyedited and formatted. The final version may differ from this version.

HEK293A cells (Invitrogen Catalog #R70507) were maintained in complete DMEM supplemented with 5% FBS, 2 mM L-glutamine, 20 mM HEPES, 0.1 mM Non-Essential Amino Acids, 1 mM sodium pyruvate, at 37 °C in a humidified incubator containing 5% CO_2 and 95% O_2. Vectors encoding mApple-CaMKIIα (WT or CA) and $mGlu_{5a}$ (3 μg DNA each) or empty vector controls (3 μg) were co-tranfected into one 10-cm dish of 60-70% confluent HEK293A cells using 3 μl of Fugene 6 (Promega Catalog # E2691) per μg of DNA. About 48 hours later, cells were lysed in 50 mM Tris-HCl pH 7.5, 150 mM NaCl, 1 mM EDTA, 1 mM EGTA, 1 mM DTT, 0.5% NP-40 (v/v), 0.5% deoxycholate (v/v), 0.2 mm PMSF, 1 mm benzamidine, 10 μg/ml leupeptin, 10 μm pepstatin, and 1 μm microcystin. Cell lysates were cleared by centrifugation (10 min at 12,000 x *g*), and a 30 μL sample of the input was saved for SDS-PAGE. The remaining supernatant was incubated at 4˚C for 1 hour with rabbit anti-HA antibodies and 20 μl prewashed Dynabeads Protein A (Thermo-Fisher, Cat. #10001D, 50% v/v). Beads were isolated magnetically, washed three times using lysis buffer and eluted using 2X Laemmli sample buffer for 10 minutes at room temperature prior to SDS-PAGE and Western Blotting.

Biotinylation and cell surface expression

Transfected HEK293A cells (see above) were placed on ice, the media was gently removed and the cells were immediately washed two times using ice cold PBS. Cells were then scraped into ice-cold PBS, transferred to a 1.5 mL tube, centrifuged at 4°C (500 x *g*; 3 min), and gently resuspended in 1 mL of cold PBS containing 2 mg of EZ-Link Sulfo-NHS-SS-Biotin. After gently rocking for 1 hour, excess reagent was quenched by addition of 50 mM Tris HCl pH 8.0, and cells were centrifuged and washed again in 1 mL of 50 mM Tris HCl. Cells were then suspended in 1 mL of ice-cold lysis buffer (25 mM Tris HCl, pH 7.4, 150 mM NaCl, 1% NP-40,

Molecular Pharmacology Fast Forward. Published on October 3, 2018 as DOI: 10.1124/mol.118.113142
This article has not been copyedited and formatted. The final version may differ from this version.

0.5% sodium deoxycholate containing 0.2 mm PMSF, 1 mm benzamidine, 10 μg/ml leupeptin, and 10 μm pepstatin), and incubated on ice for 30 min. Insoluble material was removed by centrifugation (16,000 x *g*; 10 min, 4°C) and a 30 μL aliquot of the supernatant was saved for an input sample for SDS-PAGE (Cho et al., 2014). The remaining supernatants were mixed for 1 hour at 4°C with magnetic NeutrAvidin beads (30 μL; 50% slurry). The beads were separated magnetically and washed three times with lysis buffer. Biotinylated proteins were dissociated from the beads in SDS sample buffer containing 150 mM DTT for 10 minutes at room temperature. The biotinylated and total protein samples were analyzed by Western blotting for $mGlu_5$.

Immunoblotting and semi-quantitative analysis

Since heating samples results in aggregation of full-length $mGlu_5$ protein, all samples that were blotted for the full-length receptor were eluted in SDS sample buffer containing 150 mM DTT for 10 minutes at room temperature before SDS-PAGE. SDS-polyacrylamide gels were transferred to nylon-backed nitrocellulose membranes in 10 mM CAPS buffer. After blocking in TTBS (50 mm Tris-HCl, pH 7.5, 0.1% (v/v) Tween 20, 150 mm NaCl) containing 5% nonfat milk, membranes were incubated for either 2 h at room temperature for purified protein studies or overnight at 4 °C in HEK293A and brain lysate samples with primary antibodies diluted in TTBS with 5% milk. Membranes were washed 5 times in TTBS and incubated for 1 h at room temperature with secondary antibodies conjugated to horseradish peroxidase (Promega or Santa Cruz Biotechnology), or infrared dyes (LiCor Biosciences, Lincoln, NE) diluted in TTBS with 5% milk. Antibody signals were visualized via enzyme-linked chemiluminescence using the Western Lightening Plus-ECL, enhanced chemiluminescent substrate (PerkinElmer) and

Molecular Pharmacology Fast Forward. Published on October 3, 2018 as DOI: 10.1124/mol.118.113142
This article has not been copyedited and formatted. The final version may differ from this version.

visualized using Premium X-ray Film (Phenix Research Products). Images were quantified using ImageJ software. Secondary antibodies conjugated to infrared dyes (LI-COR Biosciences) were used for development with an Odyssey system (LI-COR Biosciences).

Antibodies

The following antibodies were used for immunoblotting at the indicated dilutions: Total CaMKIIα (Thermo Catalog # MA1-048 1:5000) and p-Thr286 CaMKIIα (Santa Cruz Biotechnology Catalog # sc-12886-R, 1:3000), $mGlu_5$–specific antibody (Millipore, Catalog # AB5675, 1:3000), rabbit anti-HA (Santa Cruz, Catalog #sc805, 5 uL for immunoprecipitation), goat-GST antibody (Abcam Catalog # ab181652, 1:10,000).

Secondary antibodies: HRP-conjugated anti-rabbit (Promega catalog #W4011, 1:3000), HRP-conjugated anti-mouse (Promega catalog #W4021, 1:3000), and HRP-conjugated anti-goat (Santa Cruz Biotechnology catalog #sc-2056, 1:3000), IR dye-conjugated donkey anti-rabbit 800CW (LI-COR Biosciences catalog #926–32213, 1:10,000), and IR dye-conjugated donkey anti-mouse 680LT (LI-COR Biosciences catalog #926–68022, 1:10,000).

Mice

CaMKII-KO mice were generated in the Vanderbilt Transgenic Mouse Core as a by-product of published CRISPR/Cas9 mediated experiments directed at creating a knock-in E183V mutation of CaMKIIα (Stephenson et al., 2017). We selected a founder containing a deletion of 11-base pairs (TGCTGAGGAAG) from exon 8, leading to a frame shift and early translational termination. The knockout of CaMKIIα was confirmed by Western Blot. Primers used to genotype the CaMKIIα knockout mice are: (Forward) 5'GATACCTCTCCCCAGAAGGAC3', (Reverse) 5'TGCAGTGGTAAGGAGTGGTG3' for wild-type and (Forward)

Molecular Pharmacology Fast Forward. Published on October 3, 2018 as DOI: 10.1124/mol.118.113142
This article has not been copyedited and formatted. The final version may differ from this version.

5'GGACAGTACAACCCCAGCTT3' and (Reverse) 5'CCCGTACGGGTCCTTCCTCA3' for knockout generating a 206bp band for WT, 351bp band for KO, and 557bp band for all mice and the CaMKIIα-KO was confirmed by immunoblotting brain lysates. All mice were on a mixed B6D2 (C57BL/6J (B6) x DBA/2J (D2)) background and were housed (2–5 per cage) on a 12 h light-dark cycle with food and water *ad libitum*. Wild-type and knockout experimental mice (littermates) were generated using a HETXHET breeding strategy. All animal procedures were approved by the Vanderbilt University Institutional Animal Care and Use Committee in accordance with the National Institutes of Health *Guide for the care and use of laboratory animals*.

Mouse brain tissue preparation and immunoprecipitation

Both male and female mice were anesthetized with isofluorane, decapitated, and forebrains were quickly dissected. Half of a forebrain (cut along the mid-line) was homogenized using at least 20 strokes with a Dounce homogenizer in 1.5 mL of an isotonic buffer containing 150 mM KCl, 50 mM Tris-HCl, 1 mm DTT, 1% (v/v) Triton X-100, 1% sodium deoxycholate, 0.2 mM PMSF, 1 mM benzamidine, 10 μg/ml leupeptin, 10 μM pepstatin, and 1 μM microcystin. The homogenate was rotated end-over-end at 4°C for 30 min and then centrifuged at 10,000 × *g* for 30 min to remove insoluble material. A 30μL input sample was saved before CaMKIIα (MA1-048) antibody and 20μL magnetic Protein G beads (Invitrogen Catalog #10003D) was added to 1 mL of homogenate and rotated end over end for 3-4 hours. Beads were separated magnetically and washed three times with homogenization buffer. Immunoprecipitated complexes were eluted using 2X Lamelli Sample Buffer containing 150 mM DTT for 10 minutes at room temperature. CaMKII and $mGlu_5$ immunoprecipitation was analyzed by immunoblot analysis.

Molecular Pharmacology Fast Forward. Published on October 3, 2018 as DOI: 10.1124/mol.118.113142
This article has not been copyedited and formatted. The final version may differ from this version.

Ca^{2+} Imaging in 96-well Plates

A FlexStation II liquid handler/plate reader (Molecular Devices) was used for intracellular Ca^{2+} measurements in HEK293A cells stably expressing low amounts of the rat $mGlu_{5a}$ receptor (*293A-5a^{LOW}* cells) as previously described (Gregory et al., 2012; Hammond et al., 2010; Noetzel et al., 2012). The cells were maintained at 37°C in complete DMEM supplemented with 10% fetal bovine serum, 2 mM l-glutamine, 20 mM HEPES pH 7.5, 0.1 mM nonessential amino acids, 1 mM sodium pyruvate, antibiotic/antimycotic solution (Invitrogen), and 500 µg/ml G418, in a humidified incubator containing 5% CO_2/95% O_2. For experiments, 10 cm dishes were transfected with 3 µg of mApple control vector (mApp) or 3 µg mApp-CaMKIIα (wild type or CA; see above). The following day, cells were transferred to clear-bottomed, black-walled, poly(d-lysine)-coated 96-well plates (BD BioCoat, Bedford, MA) (3×10^4 cells per well) in DMEM containing 10% dialyzed FBS, 20 mM HEPES, 1 mM sodium pyruvate, and incubated overnight at 37°C in 5% CO_2. Approximately 24 hours later, medium was manually removed and replaced with Hanks' balanced salt solution containing 20 mM HEPES, 2.5 mM probenecid, and 2 µM Fluo-4/acetoxymethyl ester dye, pH 7.4, and plates were incubated for 30 min (37°C, 5% CO_2). This medium was manually removed and replaced with 40 µl of calcium assay buffer (Hanks' balanced salt solution, 20 mM HEPES, and 2.5 mM probenecid, pH 7.4). Glutamate additions were performed after a 30 s baseline to construct concentration-response curves (CRCs) and plates were monitored for a total of 120 sec using an excitation wavelength of 488 nm, an emission wavelength of 525 nm, and a cutoff wavelength of 515 nm. Data were collected with SoftMax Pro (Molecular Devices) then transformed and agonist concentration-response curves were fitted to a four-parameter logistic equation with GraphPad Prism. For area under the

Molecular Pharmacology Fast Forward. Published on October 3, 2018 as DOI: 10.1124/mol.118.113142
This article has not been copyedited and formatted. The final version may differ from this version.

curve measurements, time parameters were set to measure the area under the curve between the timepoints of 10-60 seconds to capture the initial Ca^{2+} peak. Raw values were generated by SoftMax Pro and normalized to the max response of control cells.

Single Cell Ca^{2+} Imaging

HEK293A cells were transiently transfected to express full-length $mGlu_{5a}$ (WT or AAA: 0.3µg DNA) and either mApple or mApple-CA-CaMKIIα (3 µg DNA). The following day, transfected cells were plated in clear glass-bottomed, poly(D-lysine)-coated 29 mM dishes (Cellvis D29-10-1.5-N) (5×10^4 cells) in DMEM containing 10% dialyzed FBS, 20 mM HEPES, 1 mM sodium pyruvate, and 1% Pennicillin/Streptomycin (Gibco) and incubated overnight at 37°C in 5% CO_2. The day of the experiment, cells were incubated in media supplemented with 2 µM Fura-2 acetoxymethyl ester (Molecular Probes) for 20 minutes at 37°C in 5% CO_2, and then transferred to Ca^{2+} imaging solution (150 mM NaCl, 5 mM KCl, 2 mM $CaCl_2$, 2 mM $MgCl_2$, 10 mM glucose and 10 mM HEPES pH 7.5 (~313 mOsm)). After incubation for 20 minutes at 37°C in 5% CO_2, fluorescence imaging was performed using a Nikon Eclipse TE2000-U microscope equipped with an epifluorescence illuminator (Sutter, Inc), a CCD camera (HQ2; Photometrics Inc), and Nikon Elements software. Cells were perfused at 37°C at a flow of 2 mL/min with Ca^{2+} imaging solution. First, the field of view was imaged using 568 nm excitation to detect cells expressing either mApple-CA-CaMKII or mApp-PCDNA3.1 control. Then, ratios of emitted fluorescence (at 510 nm) from mApple positive cells were measured following excitation at 340 nm and 380 nm (F340/F380); ratios were measured every 3 seconds for a 1 min baseline period. Thn the cells were treated with 100 µM glutamate (added to the Ca^{2+} imaging solution) for 10 min during which the FURA2 F340/F380 ratios were collected every 3 s. Relative changes in

Molecular Pharmacology Fast Forward. Published on October 3, 2018 as DOI: 10.1124/mol.118.113142
This article has not been copyedited and formatted. The final version may differ from this version.

Ca^{2+} of the mApple expressing cells were analyzed using Nikon Elements software. The F340/F380 ratios of each cell were normalized to the first F340/F380 ratio acquired for that cell during the baseline period (F/F0 = (340/380 value)/(baseline 340/380 value)) and then analyzed using Clampfit software (Molecular Devices, Sunnyvale, California). Peak Ca^{2+} responses for all cells were aligned (at 45 seconds), a ROUT test was first used to identify outliers in the maximal ΔF/F0 values for all cells within each experimental group, and then ΔF/F0 values for each time point were averaged together for each dish of cells. The maximal Ca^{2+} response (Max Peak) was defined as the average of all the peak ΔF/F0 values on an experimental day. An average trace for each day of experiments was generated to calculate the half-life of each condition. To compare half-lives of the Ca^{2+} signals the decline of the average ΔF/F0 values in each dish were normalized to the average max peak in that dish, and then fitted to a non-linear one phase exponential decay fit constrained to y0 = 1 using Graphpad Prism software (version 6.0). We determined ΔF/F0 and half lives in 5 independent experiments (transfections) on separate days (19-124 cells per condition per day) and tested for differences using a Student's T-Test. All values are presented as the mean ± SEM.

Results

Mouse forebrain lysates contain CaMKIIα-mGlu$_5$ complexes

In order to confirm that mGlu$_5$ specifically associates with CaMKII in the brain, we incubated forebrain lysates from WT or CaMKIIα-KO mice with a CaMKIIα-specific monoclonal antibody or a control IgG. The resulting immune complexes were isolated and then immunoblotted for mGlu$_5$ and CaMKIIα. Note that the mGlu$_5$ antibody used for these studies recognizes an epitope

Molecular Pharmacology Fast Forward. Published on October 3, 2018 as DOI: 10.1124/mol.118.113142
This article has not been copyedited and formatted. The final version may differ from this version.

that is shared by the two known $mGlu_5$ splice variants, $mGlu_{5a}$ and $mGlu_{5b}$, which are differentially expressed during development (Minakami et al., 1995; Romano et al., 1996). Input samples from WT and CaMKIIα-KO tissue prepared in parallel contain similar levels of the monomeric and dimeric forms of $mGlu_5$ (Figure 1), although the ratio of monomeric and dimeric species varied between independent experiments (not shown). CaMKIIα complexes isolated from WT mouse forebrain contained both monomeric and dimeric forms of $mGlu_5$, with the ratio of these forms reflecting variability in the ratio detected in the inputs. However, very little $mGlu_5$ could be detected in IgG control complexes isolated from WT tissue, or in CaMKIIα complexes isolated from CaMKIIα-KO tissue (Figure 1). Thus, $mGlu_5$ is a *bona fide* component of the CaMKIIα complexes present in mouse brain lysates.

CaMKIIα directly binds to the $mGlu_5$ C-terminal domain

Like most prior studies, we chose to use the $mGlu_{5a}$ splice variant for our molecular studies. It was previously reported that residues 827-964 of the $mGlu_{5a}$-CTD bind to inactive CaMKIIα, but that CaMKII autophosphorylation disrupted the interaction (Jin et al., 2013b). In order to confirm this finding, we generated a GST-tagged $mGlu_{5a}$ CTD construct containing residues 827-964 (GST-$mGlu_{5a}$-CTD) for use in glutathione agarose co-sedimentation experiments. Initial studies detected weak binding of inactive CaMKIIα to GST-$mGlu_{5a}$-CTD that was not consistently above background binding to a GST negative control (data not shown). Therefore, we systematically tested interactions of GST-$mGlu_{5a}$-CTD with CaMKIIα in various activation states.

Purified CaMKIIα was autophosphorylated in the presence of Ca^{2+}/CaM *in vitro* at either 4°C or at 30°C. Similar total levels of Thr286 autophosphorylation were detected by immunoblotting

Molecular Pharmacology Fast Forward. Published on October 3, 2018 as DOI: 10.1124/mol.118.113142
This article has not been copyedited and formatted. The final version may differ from this version.

following incubation at either 4°C or at 30°C (Figure 2A), but the 30°C autophosphorylation reduced the electrophoretic mobility of CaMKIIα. These observations are consistent with prior studies showing that incubation at 4°C results in selective Thr286 autophosphorylation (McNeill and Colbran, 1995), whereas incubation at 30°C allows for extensive autophosphorylation at several other sites (Baucum et al., 2015).

We then performed glutathione-agarose cosedimentation experiments to test the interaction of GST-mGlu$_5$-CTD with CaMKIIα in these different activation states (after terminating the autophosphorylation reactions by chelating metal ions with excess EGTA and EDTA). The selective Thr286-autophosphorylation (4°C) protocol resulted in a robust enhancement of CaMKIIα binding to GST-mGlu$_5$-CTD relative to the non-phosphorylated kinase, but this interaction was substantially reduced following more extensive *in vitro* phosphorylation at 30°C (Figure 2B). The short exposure times used for development of these immunoblots failed to detect weak binding of inactive CaMKIIα to GST-mGlu$_5$-CTD. In combination, these data show that while activation and Thr286 autophosphorylation of CaMKIIα strongly enhances binding to the mGlu$_{5a}$ CTD, the interaction can be weakened by autophosphorylation at additional non-Thr286 sites.

Binding of activated CaMKIIα to the GST-mGlu$_{5a}$ CTD is disrupted by Ca^{2+}/CaM

Ca^{2+}/CaM binds to residues 889-917 within the CTD of mGlu$_{5a}$ with important functional consequences (Choi et al., 2011; Lee et al., 2008; Minakami et al., 1997). Moreover, it was previously reported that excess Ca^{2+}/CaM disrupts the binding of inactive CaMKIIα to the mGlu$_{5a}$-CTD (Jin et al., 2013b). Therefore, we tested whether excess Ca^{2+}/CaM also disrupts the binding of activated CaMKIIα to GST-mGlu$_{5a}$-CTD. Thr286-autophosphorylated CaMKIIα (4°C

Molecular Pharmacology Fast Forward. Published on October 3, 2018 as DOI: 10.1124/mol.118.113142
This article has not been copyedited and formatted. The final version may differ from this version.

protocol) robustly binds to GST-mGlu$_{5a}$-CTD, as noted above, but this interaction was essentially eliminated by inclusion of excess Ca^{2+}/CaM in the binding assay (Figure 2C). Thus, binding of activated CaMKIIα to the mGlu$_{5a}$-CTD is also blocked by Ca^{2+}/CaM, suggesting that multiple Ca^{2+} sensitive proteins are involved in the regulation of mGlu$_5$ signaling.

Identification of a CaMKIIα-binding determinant in the mGlu$_5$-CTD

As an initial approach to identify key CaMKIIα binding determinants in the mGlu$_{5a}$-CTD, we compared residues 827-964 of mGlu$_5$ with CaMKIIα-binding domains that have been previously identified in other proteins. Our lab recently showed that activated CaMKIIα binds to the N-terminal domains of Cav1.2 and Cav1.3 L-type voltage gated Ca^{2+} channels, and that this interaction is disrupted by mutation of three basic residues (Arg^{83}-Lys-Arg^{85}) to alanine (Wang et al., 2017). Similar tri-basic residue motifs are also present within CaMKIIα binding domains that have been previously identified in the intracellular loops of the D_2 and D_3 dopamine receptor (Liu et al., 2009; Zhang et al., 2014), and the mGlu$_1$-CTD (Jin et al., 2013a). Notably, the CaMKIIα-binding fragment of the mGlu$_{5a}$-CTD also contains a tribasic residue motif (residues Lys^{866}-Arg^{867}-Arg^{868}) (Figure 3A). We found that substituting alanines for Lys^{866}-Arg^{867}-Arg^{868} in the mGlu$_{5a}$-CTD essentially abolished the binding of activated CaMKIIα to GST-mGlu$_5$-CTD *in vitro* (Figure 3B). These data identify a key determinant for CaMKII-binding to the CTD of mGlu$_{5a}$.

CaMKIIα activation increases CaMKIIα-mGlu$_{5a}$ association in heterologous cells

In order to better understand the interaction of CaMKIIα with full-length mGlu$_{5a}$ we conducted co-immunoprecipitation experiments from lysates of transfected HEK293A cells. We first tested

Molecular Pharmacology Fast Forward. Published on October 3, 2018 as DOI: 10.1124/mol.118.113142
This article has not been copyedited and formatted. The final version may differ from this version.

the hypothesis that CaMKIIα activation would increase the association with full-length $mGlu_{5a}$, as with *in vitro* binding of CaMKIIα to GST-$mGlu_{5a}$-CTD. We expressed mApple-tagged WT CaMKIIα in the absence or presence of $mGlu_{5a}$ with an N-terminal HA-epitope tag in HEK293A cells. Prior to HA immunoprecipitation, the cell lysates were split into two aliquots and pre-incubated with either excess EGTA and EDTA or with Ca^{2+}/CaM, Mg^{2+}, ATP, and phosphatase inhibitors to stimulate CaMKIIα autophosphorylation. CaMKII activation in the lysates resulted in a robust increase in autophosphorylation at Thr286, without the large shift in electrophoretic mobility that was observed following autophosphorylation of purified CaMKIIα at 30°C (Figure 4A). HA-immununoprecipitation from the two preincubated lysates yielded similar amounts of the monomeric and dimeric species of HA-$mGlu_{5a}$, but CaMKIIα activation resulted in a statistically significant ~3-fold increase in the amount of co-immunoprecipitated CaMKIIα (Figure 4A). These data show that full-length $mGlu_{5a}$ preferentially interacts with activated WT CaMKIIα.

Association of activated CaMKIIα with full-length $mGlu_{5a}$ requires Arg^{83}-Lys-Arg^{85}

We next investigated whether the association of activated CaMKIIα with full-length $mGlu_{5a}$ involves the CTD. In order to avoid complications that might arise from preincubating cell lystates to activate WT-CaMKIIα, we used an mApple-tagged constitutively active T286D/T305A/T306A triple mutant of CaMKIIα (mApple-CA-CaMKIIα); the phospho-mimetic T286D mutation results in constitutive CaMKIIα activity and the phospho-null T305A/T306A mutations prevent CaMKIIα phosphorylation at these sites, which interferes with binding of Ca^{2+}/CaM and α-actinin (Jalan-Sakrikar et al., 2012). The mApple-CA-CaMKIIα was expressed alone, or co-expressed with either HA-$mGlu_{5a}$ or HA-$mGlu_{5a}$-AAA (with Lys^{866}-Arg^{867}-Arg^{868}

Molecular Pharmacology Fast Forward. Published on October 3, 2018 as DOI: 10.1124/mol.118.113142
This article has not been copyedited and formatted. The final version may differ from this version.

mutated to alanines). HA-immunoprecipitation from cell lysates confirmed a robust association of mApple-CA-CaMKIIα with WT $mGlu_{5a}$ that was partially (~50%) reduced by the triple alanine mutation in the CTD (Figure 4B). These data demonstrate that the Lys^{866}-Arg^{867}-Arg^{868} residues in the $mGlu_{5a}$-CTD play an important role in the association of activated CaMKIIα with the full-length $mGlu_5$ receptor.

CaMKIIα increases basal $mGlu_{5a}$ surface expression

Since the CTD is known to modulate $mGlu_5$ cell surface expression and consequently $mGlu_5$ signaling, we investigated the effect of CaMKIIα on the cell-surface expression of full-length $mGlu_{5a}$. Intact HEK293A cells expressing $mGlu_5$ with or without mApple-CA-CaMKIIα were incubated with Sulfo-NHS-SS-Biotin to biotinylate all surface-expressed proteins. Streptavidin-conjugated magnetic beads were then used to isolate cell-surface proteins from cell lysates. Immunoblototting of total cell lysates and isolated cell-surface proteins revealed that the co-expression of mApple-CA-CaMKIIα increased the proportion of $mGlu_{5a}$ expressed on the cell-surface by 3.0±0.7-fold (SEM) under basal conditions ($p=0.036$; one-sample t-test vs. hypothetical value of 1) (Figure 5). In order to determine whether CaMKIIα interaction with the $mGlu_{5a}$ CTD is important for this effect we examined the cell surface expression of $mGlu_{5a}$-AAA, in which Lys^{866}-Arg^{867}-Arg^{868} in the CTD were replaced with alanines. In the absence of co-expressed CaMKII, the surface expression of $mGlu_{5a}$-AAA was not significantly different from those of WT $mGlu_{5a}$ (1.6±0.6-fold (SEM); $n= 5$; $p=0.35$; one-sample t-test vs. hypothetical value of 1). Moreover, the co-expression of mApple-CA-CaMKIIα had no effect on cell-surface expression of $mGlu_{5a}$-AAA. These data demonstrate that interaction with the $mGlu_{5a}$-CTD is necessary for CaMKIIα-mediated increases in $mGlu_{5a}$ cell-surface expression.

Molecular Pharmacology Fast Forward. Published on October 3, 2018 as DOI: 10.1124/mol.118.113142
This article has not been copyedited and formatted. The final version may differ from this version.

CaMKIIα reduces $mGlu_{5a}$-stimulated peak Ca^{2+} mobilization

To investigate the effect of CaMKIIα on $mGlu_{5a}$ signaling, we measured glutamate-induced Ca^{2+} mobilization in populations of 293A-$5a^{LOW}$ cells that stably express $mGlu_{5a}$ and were transiently transfected to co-express mApple or mApple-tagged CaMKIIα (either WT or CA). A similar fraction of the total cells expressed detectable levels of mApple-tagged WT- or CA-CaMKIIα in each transfection (typically ~60%). After loading glutamate-starved cells with fluo-4-AM, a fluorescent Ca^{2+} indicator, we measured fluorescence responses of total cell populations to increasing glutamate concentrations (0.01-100 μM) (Figure 6A). An overlay of raw traces from cells expressing mApple, mApple-WT-CaMKIIα, or mApple-CA-CaMKIIα in a representative experiment is shown in Figure 6B. Peak Ca^{2+} responses (increased fluorescence) at each glutamate concentration were expressed as a ratio to the maximum response to a saturating concentration of glutamate (100 μM) in mApple-expressing control cells for each individual experiment, and then data were averaged across 5 independent experiments. Glutamate increased the peak fluorescence in a concentration-dependent manner, with an apparent EC_{50} of 0.38±0.03 μM in control cells, similar to previous analyses (Hammond et al., 2010; Schoepp et al., 1999). The glutamate response was unaffected by co-expression of mApple-WT-CaMKIIα, but the co-expression of mApple-CA-CaMKIIα reduced peak Ca^{2+} responses at the highest concentrations of glutamate by approximately 20%, without affecting the apparent EC_{50} (Figure 6C). As an alternative measure of Ca^{2+} responses, we determined the area under the curve of the initial Ca^{2+} peak at the highest glutamate concentration. There was no difference in area under the curve between cells expressing mApple or mApple-CaMKIIα-WT, but the co-expression of mApple-CA-CaMKIIα significantly reduced the area under the curve (Control, 109.2±2.7; WT,

Molecular Pharmacology Fast Forward. Published on October 3, 2018 as DOI: 10.1124/mol.118.113142
This article has not been copyedited and formatted. The final version may differ from this version.

101.3±7.4; CA, 82.6±4.1. One-way ANOVA, p=0.011, F=6.280. Sidak's *post hoc* test for multiplicity adjusted *p* values: WT vs. control, p=0.51, CA vs. control, p=0.0073) (data not shown). Since mApple-CA-CaMKIIα is expressed in only a fraction of the cell population in each well, the measured reductions in maximal Ca^{2+} responses presumably under-estimate the actual impact of expressing CA-CaMKIIα in each cell. However, these data cannot differentiate whether this effect reflects decreased Ca^{2+} mobilization within each cell or a decrease in the fraction of responsive cells. Nevertheless, the data indicate that the co-expression of CA-CaMKIIα but not WT-CaMKIIα can reduce $mGlu_{5a}$-stimulated peak Ca^{2+} mobilization.

CaMKIIα prolongs $mGlu_{5a}$-mediated Ca^{2+} signaling

To address caveats associated with studies investigating the effects of mApple-CA-CaMKIIα on Ca^{2+} mobilization in 293A-$5a^{LOW}$ cells, we also examined Ca^{2+} mobilization in single HEK293A cells transfected to express full-length $mGlu_{5a}$ with either mApple alone (control) or mApple-CA-CaMKIIα. After loading all cells with Fura-2-AM, a ratiometric Ca^{2+} indicator, single cells were selected for analysis based on the presence of mApple as a marker of transfection. Application of 100 μM glutamate to cells co-expressing soluble mApple or mApple-CA-CaMKIIα with WT $mGlu_{5a}$ produced an initial peak of Fura-2 fluorescence followed by highly variable changes of fluorescence over the next 10 min (Figure 7A). In a majority of cells in each group (53-68%) Ca^{2+} signals waned over time, sometimes with a secondary shoulder, but subpopulations of the cells displayed clear Ca^{2+} oscillations that either returned to baseline between oscillations (10-21%) or were super-imposed on a more sustained Ca^{2+} elevation (18-25%) (Supplemental Figure 1A-C). However, the percentage of WT $mGlu_{5a}$ cells exhibiting Ca^{2+} oscillations was unaffected by the co-expression of mApple-CA-CaMKIIα (Supplemental Figure

Molecular Pharmacology Fast Forward. Published on October 3, 2018 as DOI: 10.1124/mol.118.113142
This article has not been copyedited and formatted. The final version may differ from this version.

1D). Since it is unclear whether oscillating and non-oscillating cells have different physiological effects, we developed an approach to analyze the responses of all cells (both oscillating and non-oscillating) across 5 independent experiments, revealing that the initial peak fluorescence was significantly reduced ($p=0.009$) in cells expressing mApple-CA-CaMKIIα vs. cells expressing mApple alone (Figure 7B), consistent with data from stably transfected cell populations (Figure 6). Moreover, the Ca^{2+} signal was relatively prolonged in cells expressing mApple-CA-CaMKIIα vs. cells expressing mApple alone, as reflected by a statistically-significant increase in the half-life of the fluorescence signal (Figure 7A inset, 7C). We also analyzed responses in subsets of the cells within each population that exhibited at least three baseline Ca^{2+} oscillations (Supplemental Figure 2A). There was no statistically significant difference in the total number of $mGlu_{5a}$-mediated Ca^{2+} oscillations between transfection conditions (Supplemental Figure 2B). However, co-expression of mApple-CA-CaMKIIα reduced the relative rate of decay of peak Ca^{2+} signals in successive oscillations (Supplemental Figure 2C). Co-expression of mApple-CA-CaMKIIα also increased the frequency of Ca^{2+} oscillations, as reflected by a reduction of the inter-event intervals (Supplemental Figure 2D). In combination, these data indicate that CaMKIIα can reduce the amplitude of initial $mGlu_{5a}$-dependent Ca^{2+} mobilization while extending the relative duration of Ca^{2+} signals and increasing the frequency of oscillations when they are present.

To test the hypothesis that CaMKIIα binding to the $mGlu_{5a}$-CTD is necessary for the modulation of Ca^{2+} mobilization, we examined the effect of co-expressing mApple-CA-CaMKIIα with $mGlu_{5a}$-AAA, in which Lys^{866}-Arg^{867}-Arg^{868} in the CTD were replaced with alanines (Figure 7D). This CTD mutation had little effect on glutamate-stimulated Ca^{2+} mobilization in cells expressing mApple. Moreover, the co-expression of mApple-CA-CaMKIIα with $mGlu_{5a}$-AAA

Molecular Pharmacology Fast Forward. Published on October 3, 2018 as DOI: 10.1124/mol.118.113142
This article has not been copyedited and formatted. The final version may differ from this version.

had no statistically significant effect on either the initial peak (Figure 7E) or the duration (Figure 7F) of the glutamate-stimulated Ca^{2+} signal relative to control cells expressing mApple alone. Furthermore, the CTD mutation had no statistically significant effect on the responses of cells displaying baseline Ca^{2+} oscillations (Supplementary Figure 1D), but abrogated the CaMKII-dependent modulation, as reflected by a lack of effect on the peak height decay of successive Ca^{2+} oscillations (Supplemental Figure 2C) and the Ca^{2+} oscillation frequency (Supplemental Figure 2D). These data indicate that binding to the $mGlu_{5a}$-CTD is important for both the increase of initial peak Ca^{2+} signals and for the prolonged Ca^{2+} signaling induced by co-expression of CA-CaMKIIα.

Discussion

In a previous report, the membrane proximal region of the $mGlu_{5a}$-CTD was shown to bind *inactive* CaMKII (Jin et al., 2013b). Here we extend these findings by further characterizing the physical and functional relationship between these key regulators of synaptic transmission. We confirmed that CaMKIIα and $mGlu_5$ specifically interact in mouse brain. However, our data show that $mGlu_{5a}$-CTD residues 827-964 bind more strongly to CaMKIIα in an active, Thr286-autophosphorylated conformation, but that this interaction is disrupted by excess Ca^{2+}/CaM or by robust CaMKII autophosphorylation at additional undefined sites. Furthermore, our data indicate that CaMKII binding to the CTD exerts complex effects on $mGlu_{5a}$ surface expression and downstream Ca^{2+} mobilization.

There is a growing appreciation that specific physiological actions of CaMKII are modulated in part through dynamically-regulated interactions with CaMKII-associated proteins (CaMKAPs). Several CaMKAPs preferentially interact with activated conformations of CaMKII; these

Molecular Pharmacology Fast Forward. Published on October 3, 2018 as DOI: 10.1124/mol.118.113142
This article has not been copyedited and formatted. The final version may differ from this version.

CaMKAPs can be sub-classified based on differences between the amino acid sequences of their CaMKII-binding domains. CaMKII-binding domains in the NMDA receptor GluN2B subunits and calcium channel β1 and β2 subunits resemble the CaMKII regulatory domain (Grueter et al., 2008; Strack et al., 2000). In contrast, the amino acid sequence of a CaMKII-binding domain in densin has similarity with a naturally occurring CaMKII inhibitor protein (CaMKIIN) (Jiao 2011). Here, we show here that the binding domain for activated CaMKII in the $mGlu_{5a}$ CTD does not resemble these CaMKAPs. Rather, this novel interaction requires three basic residues (Lys^{866}-Arg^{867}-Arg^{868}), similar to the recently identified interaction of activated CaMKII with the N-terminal domains of L-type voltage-gated Ca^{2+} channels (Wang et al., 2017). Interestingly, triple basic residue motifs can also be identified in CaMKII-binding domains of other GPCRs, including intracellular loops of the $G\alpha_i$-coupled D_2 and D_3 dopamine receptors (Zhang et al., 2014; Liu et al., 2009), and the CTD of the $mGlu_1$ receptor (Jin et al., 2013a; Jin et al., 2013b), which also couples to $G\alpha_{q/11}$ (Figure 3). Thus, it will be interesting to investigate the role of these triple basic residue motifs in CaMKII binding to additional GPCRs.

One unusual aspect of CaMKII binding to the $mGlu_{5a}$-CTD is that, while the *in vitro* interaction requires CaMKIIα activation and Thr286 autophosphorylation, additional autophosphorylation at non-Thr286 sites following incubation at 30°C reduces the binding. Our recent proteomics analyses of purified CaMKIIα autophosphorylated *in vitro* using a similar 30°C protocol detected 17 autophosphorylation sites, in addition to Thr-286 (Baucum et al., 2015). Presumably the autophosphorylation at one or more of these non-Thr286 sites interferes with *in vitro* CaMKIIα binding to $mGlu_{5a}$. While this is a potentially interesting finding, parallel proteomics analyses of CaMKII isolated from mouse brain failed to detect phosphorylation at many of these *in vitro* sites (Baucum et al., 2015). However, it is possible that this observation explains why Jin and

Molecular Pharmacology Fast Forward. Published on October 3, 2018 as DOI: 10.1124/mol.118.113142
This article has not been copyedited and formatted. The final version may differ from this version.

colleagues found that autophosphorylated CaMKII did not bind to $mGlu_{5a}$ *in vitro* (Jin et al., 2013b) because their autophosphorylation reactions were incubated at 30°C.

Our data show that CaMKIIα activation enhances the association with full-length $mGlu_{5a}$, and that this interaction involves the Lys^{866}-Arg^{867}-Arg^{868} motif in the CTD (Figure 3). However, triple alanine substitution of CTD residues 866-868 reduced the interaction by only ~50%, suggesting that CaMKII may interact with additional regions in $mGlu_{5a}$ or bind to the receptor through an indirect interaction. Indeed, a CaMKII interaction with the second intracellular loop of $mGlu_5$ has been previously reported (Raka et al., 2015), although we have been unable to detect direct binding of purified CaMKII to a GST fusion protein containing the $mGlu_5$ second intracellular loop (data not shown). Although our data cannot preclude a role for a secondary or indirect interaction, our analyses in heterologous cells indicate that CaMKIIα interaction with the CTD is critical for several novel functional effects of CaMKII on $mGlu_{5a}$ signaling. First, we show here that CaMKIIα can increase cell surface expression of $mGlu_{5a}$. Second, we found that CaMKIIα has complex effects on $mGlu_{5a}$-dependent Ca^{2+} mobilization. As noted previously, $mGlu_5$ activation can induce temporally-diverse intracellular Ca^{2+} responses in heterologous cells and in neurons (Flint et al., 1999; Jong and O'Malley, 2017; Kim et al., 2005; Mao and Wang, 2003b; Uematsu et al., 2015). The co-expression of CaMKII had little effect on the proportion of cells exhibiting different oscillatory or non-oscillatory response patterns (Supplementary Figure 1). However, we found that the co-expression of CA-CaMKIIα reduces the amplitude of the initial peak Ca^{2+} signals (Figure 6C, Figure 7B), but prolongs the duration of the Ca^{2+} signals (Figure 7C, Supplementary Figure 2C) in both the total responding cell population or only in cells that exhibit baseline Ca^{2+} oscillations. The co-expression of CA-CaMKIIα also increases the frequency of baseline Ca^{2+} oscillations (Supplementary Figure 2D). All of these effects are

Molecular Pharmacology Fast Forward. Published on October 3, 2018 as DOI: 10.1124/mol.118.113142
This article has not been copyedited and formatted. The final version may differ from this version.

prevented by the triple alanine substitution for Lys^{866}-Arg^{867}-Arg^{868} in the CTD (Figure 7D-F, Supplementary Figure 2C,D). Presumably, the effect of CaMKIIα to increase basal cell-surface expression contributes to the prolongation of Ca^{2+} signaling, but the mechanisms underlying the reduced initial peak Ca^{2+} signal, observed in both stable 293A-5a^{LOW} cell populations and in single transiently-transfected cells, remains unclear. Taken together, our data show that binding of CaMKIIα can play an important role in modulating cellular responses to $mGlu_{5a}$ activation. Further examination into the contribution of these mechanisms in synaptic plasticity and neuronal Ca^{2+} signaling are warranted in future studies.

Interestingly, cell surface expression of $mGlu_{5a}$ is also modulated by direct binding of Ca^{2+}/CaM to the CTD, similar to the effects of CaMKIIα binding to the CTD reported herein, and Ca^{2+}/CaM also prolongs $mGlu_5$-mediated Ca^{2+} signaling (Lee et al., 2008). The Ca^{2+}/CaM binding domain involved in mediating these effects is located 30-40 residues C-terminal to the tribasic residue motif that is critical for CaMKII binding. Nevertheless, we found that Ca^{2+}/CaM competes for binding of activated CaMKII to the $mGlu_{5a}$-CTD *in vitro* (Figure 2C). Taken together, our data suggest an intriguing model in which the binding of calmodulin might confer a relatively transient Ca^{2+}-dependent modulation of $mGlu_{5a}$ surface expression and signaling, but that increased CaMKIIα autophosphorylation at Thr286 would result in sustained binding to the CTD and longer-term modulation of $mGlu_{5a}$ surface expression and Ca^{2+} mobilization. Since Thr286 autophosphorylation of CaMKII is sensitive to changes in the source, duration, or frequency of Ca^{2+} signals originating from multiple channels (Pasek et al., 2015), such as those occurring during synaptic plasticity, as well as to the regulated activities of protein phosphatases, this may provide a mechanism for cross-talk with other signaling pathways.

Molecular Pharmacology Fast Forward. Published on October 3, 2018 as DOI: 10.1124/mol.118.113142
This article has not been copyedited and formatted. The final version may differ from this version.

As noted above, CaMKII has also been shown to interact with a membrane proximal region in the CTDs of $mGlu_1$ (Jin et al., 2013a), and the CaMKII-binding domain in $mGlu_1$ contains a tri-basic residue motif, similar to the motif we have here identified as being critical for CaMKII binding to the $mGlu_{5a}$-CTD. However, CaMKII was shown to desensitize $mGlu_1$ signaling whereas we found that CaMKII prolongs $mGlu_5$ signaling. This apparently differential modulation of $mGlu_1$ and $mGlu_5$ by CaMKII may contribute to their distinct neuronal roles (Mannaioni et al., 2001; Valenti et al., 2002; Volk et al., 2006). Interestingly, the effects of CaMKII on $mGlu_1$ signaling are mediated in part by phosphorylation at Thr871, which lies within the CaMKII-binding domain. Therefore, it will be interesting to investigate whether phosphorylation is required for the effects of CaMKII on $mGlu_5$ signaling, as well as the physical interaction demonstrated here.

The effects of CaMKIIα on $mGlu_{5a}$ must also interface with the known modulation of $mGlu_5$ signaling by other mechanisms. Prior studies have shown that several protein kinases modulate $mGlu_5$ via the CTD. For example, PKC phosphorylates Ser901 in the $mGlu_{5a}$ CTD to inhibit Ca^{2+}/CaM binding and antagonize the aforementioned modulation by Ca^{2+}/CaM (Lee et al., 2008). In addition, PKA phosphorylates Ser870 in $mGlu_{5a}$, prolonging Ca^{2+} mobilization, similar to the effects of CaMKII reported here, and enhancing ERK activation (Uematsu et al., 2015). However, it was previously reported that CaMKII reduces $mGlu_5$-stimulated ERK1/2 activation and increases agonist-induced $mGlu_5$ internalization (Raka et al., 2015). It is possible that the enhanced agonist-induced internalization in part results from the increased basal surface expression reported herein (Figure 5). Although the mechanistic relationships between these different modes of $mGlu_5$ regulation remain to be more clearly established, the convergence of Ca^{2+}/CaM, CaMKII, PKA and PKC actions within an ~60 amino acid region in the long CTD

Molecular Pharmacology Fast Forward. Published on October 3, 2018 as DOI: 10.1124/mol.118.113142
This article has not been copyedited and formatted. The final version may differ from this version.

(345 amino acids) suggests that the actions of $mGlu_5$ are tightly controlled across different time frames, presumably fine-tuning neuronal responses such as different forms of synaptic plasticity.

Acknowledgements: We thank Hyekyung Plumley Cho for help with Flex Station experiments We are grateful to Dr. David A. Jacobson and Prasanna Dadi for providing access to equipment for the single-cell Ca^{2+} imaging and for helpful discussions. We also thank David Piston, and Winship Herr for generously providing various plasmids, as detailed in the text.

Author Contributions:

Participated in research design: Marks, Shonesy, Wang, Niswender, Colbran

Conducted experiments: Marks

Contributed new reagents or analytic tools: Marks, Wang, Stephenson, Niswender

Performed data analysis: Marks, Shonesy

Wrote or contributed to the writing of the manuscript: Marks, Shonesy, Colbran

References:

Ade KK, Wan Y, Hamann HC, O'Hare JK, Guo W, Quian A, Kumar S, Bhagat S, Rodriguiz RM, Wetsel WC, Conn PJ, Dzirasa K, Huber KM and Calakos N (2016) Increased Metabotropic Glutamate Receptor 5 Signaling Underlies Obsessive-Compulsive Disorder-like Behavioral and Striatal Circuit Abnormalities in Mice. *Biol Psychiatry* **80**(7): 522-533.

Baucum AJ, 2nd, Shonesy BC, Rose KL and Colbran RJ (2015) Quantitative proteomics analysis of CaMKII phosphorylation and the CaMKII interactome in the mouse forebrain. *ACS Chem Neurosci* **6**(4): 615-631.

Cho HP, Garcia-Barrantes PM, Brogan JT, Hopkins CR, Niswender CM, Rodriguez AL, Venable DF, Morrison RD, Bubser M, Daniels JS, Jones CK, Conn PJ and Lindsley CW (2014) Chemical modulation of mutant mGlu1 receptors derived from deleterious GRM1 mutations found in schizophrenics. *ACS Chem Biol* **9**(10): 2334-2346.

Choi KY, Chung S and Roche KW (2011) Differential binding of calmodulin to group I metabotropic glutamate receptors regulates receptor trafficking and signaling. *J Neurosci* **31**(16): 5921-5930.

Coultrap SJ, Freund RK, O'Leary H, Sanderson JL, Roche KW, Dell'Acqua ML and Bayer KU (2014) Autonomous CaMKII mediates both LTP and LTD using a mechanism for differential substrate site selection. *Cell Rep* **6**(3): 431-437.

Enz R (2012) Structure of metabotropic glutamate receptor C-terminal domains in contact with interacting proteins. *Front Mol Neurosci* **5**: 52.

Flint AC, Dammerman RS and Kriegstein AR (1999) Endogenous activation of metabotropic glutamate receptors in neocortical development causes neuronal calcium oscillations. *Proceedings of the National Academy of Sciences* **96**(21): 12144-12149.

Foster DJ and Conn PJ (2017) Allosteric Modulation of GPCRs: New Insights and Potential Utility for Treatment of Schizophrenia and Other CNS Disorders. *Neuron* **94**(3): 431-446.

Giese KP, Fedorov NB, Filipkowski RK and Silva AJ (1998) Autophosphorylation at Thr286 of the alpha calcium-calmodulin kinase II in LTP and learning. *Science* **279**(5352): 870-873.

Gregory KJ, Noetzel MJ, Rook JM, Vinson PN, Stauffer SR, Rodriguez AL, Emmitte KA, Zhou Y, Chun AC, Felts AS, Chauder BA, Lindsley CW, Niswender CM and Conn PJ (2012) Investigating metabotropic glutamate receptor 5 allosteric modulator cooperativity, affinity, and agonism: enriching structure-function studies and structure-activity relationships. *Mol Pharmacol* **82**(5): 860-875.

Grueter BA, McElligott ZA, Robison AJ, Mathews GC and Winder DG (2008) In vivo metabotropic glutamate receptor 5 (mGluR5) antagonism prevents cocaine-induced disruption of postsynaptically maintained mGluR5-dependent long-term depression. *J Neurosci* **28**(37): 9261-9270.

Hammond AS, Rodriguez AL, Townsend SD, Niswender CM, Gregory KJ, Lindsley CW and Conn PJ (2010) Discovery of a Novel Chemical Class of mGlu(5) Allosteric Ligands with Distinct Modes of Pharmacology. *ACS Chem Neurosci* **1**(10): 702-716.

Hu NW, Nicoll AJ, Zhang D, Mably AJ, O'Malley T, Purro SA, Terry C, Collinge J, Walsh DM and Rowan MJ (2014) mGlu5 receptors and cellular prion protein mediate amyloid-beta-facilitated synaptic long-term depression in vivo. *Nat Commun* **5**: 3374.

Huber KM, Roder JC and Bear MF (2001) Chemical induction of mGluR5- and protein synthesis--dependent long-term depression in hippocampal area CA1. *J Neurophysiol* **86**(1): 321-325.

Jalan-Sakrikar N, Bartlett RK, Baucum AJ, 2nd and Colbran RJ (2012) Substrate-selective and calcium-independent activation of CaMKII by alpha-actinin. *J Biol Chem* **287**(19): 15275-15283.

Jia Z, Lu Y, Henderson J, Taverna F, Romano C, Abramow-Newerly W, Wojtowicz JM and Roder J (1998) Selective abolition of the NMDA component of long-term potentiation in mice lacking mGluR5. *Learn Mem* **5**(4-5): 331-343.

Jiao Y, Robison AJ, Bass MA and Colbran RJ (2008) Developmentally regulated alternative splicing of densin modulates protein-protein interaction and subcellular localization. *J Neurochem* **105**(5): 1746-1760.

Jin D-Z, Guo M-L, Xue B, Fibuch EE, Choe ES, Mao L-M and Wang JQ (2013a) Phosphorylation and Feedback Regulation of Metabotropic Glutamate Receptor 1 by Calcium/Calmodulin-Dependent Protein Kinase II. *The Journal of Neuroscience* **33**(8): 3402-3412.

Jin D-Z, Guo M-L, Xue B, Mao L-M and Wang JQ (2013b) Differential Regulation of CaMKIIα Interactions with mGluR5 and NMDA Receptors by Ca(2+) in Neurons. *Journal of neurochemistry* **127**(5): 620-631.

Jin DZ, Xue B, Mao LM and Wang JQ (2015) Metabotropic glutamate receptor 5 upregulates surface NMDA receptor expression in striatal neurons via CaMKII. *Brain Res* **1624**: 414-423.

Joly C, Gomeza J, Brabet I, Curry K, Bockaert J and Pin JP (1995) Molecular, functional, and pharmacological characterization of the metabotropic glutamate receptor type 5 splice variants: comparison with mGluR1. *J Neurosci* **15**(5 Pt 2): 3970-3981.

Jong YI and O'Malley KL (2017) Mechanisms Associated with Activation of Intracellular Metabotropic Glutamate Receptor, mGluR5. *Neurochem Res* **42**(1): 166-172.

Kim CH, Braud S, Isaac JT and Roche KW (2005) Protein kinase C phosphorylation of the metabotropic glutamate receptor mGluR5 on Serine 839 regulates Ca2+ oscillations. *J Biol Chem* **280**(27): 25409-25415.

Lee JH, Lee J, Choi KY, Hepp R, Lee JY, Lim MK, Chatani-Hinze M, Roche PA, Kim DG, Ahn YS, Kim CH and Roche KW (2008) Calmodulin dynamically regulates the trafficking of the metabotropic glutamate receptor mGluR5. *Proc Natl Acad Sci U S A* **105**(34): 12575-12580.

Li MZ and Elledge SJ (2012) SLIC: a method for sequence- and ligation-independent cloning. *Methods in molecular biology (Clifton, NJ)* **852**: 51-59.

Liu XY, Mao LM, Zhang GC, Papasian CJ, Fibuch EE, Lan HX, Zhou HF, Xu M and Wang JQ (2009) Activity-dependent modulation of limbic dopamine D3 receptors by CaMKII. *Neuron* **61**(3): 425-438.

Luscher C and Huber KM (2010) Group 1 mGluR-dependent synaptic long-term depression: mechanisms and implications for circuitry and disease. *Neuron* **65**(4): 445-459.

Mannaioni G, Marino MJ, Valenti O, Traynelis SF and Conn PJ (2001) Metabotropic glutamate receptors 1 and 5 differentially regulate CA1 pyramidal cell function. *J Neurosci* **21**(16): 5925-5934.

Mao L and Wang JQ (2003a) Group I metabotropic glutamate receptor-mediated calcium signalling and immediate early gene expression in cultured rat striatal neurons. *Eur J Neurosci* **17**(4): 741-750.

Mao L and Wang JQ (2003b) Metabotropic glutamate receptor 5-regulated Elk-1 phosphorylation and immediate early gene expression in striatal neurons. *J Neurochem* **85**(4): 1006-1017.

Mao LM, Liu XY, Zhang GC, Chu XP, Fibuch EE, Wang LS, Liu Z and Wang JQ (2008) Phosphorylation of group I metabotropic glutamate receptors (mGluR1/5) in vitro and in vivo. *Neuropharmacology* **55**(4): 403-408.

Mao LM and Wang Q (2016) Phosphorylation of group I metabotropic glutamate receptors in drug addiction and translational research. *J Transl Neurosci* **1**(1): 17-23.

McNeill RB and Colbran RJ (1995) Interaction of autophosphorylated Ca2+/calmodulin-dependent protein kinase II with neuronal cytoskeletal proteins. Characterization of binding to a 190-kDa postsynaptic density protein. *J Biol Chem* **270**(17): 10043-10049.

Michalon A, Sidorov M, Ballard TM, Ozmen L, Spooren W, Wettstein JG, Jaeschke G, Bear MF and Lindemann L (2012) Chronic pharmacological mGlu5 inhibition corrects fragile X in adult mice. *Neuron* **74**(1): 49-56.

Miller SG, Patton BL and Kennedy MB (1988) Sequences of autophosphorylation sites in neuronal type II CaM kinase that control Ca2(+)-independent activity. *Neuron* **1**(7): 593-604.

Minakami R, Iida K, Hirakawa N and Sugiyama H (1995) The expression of two splice variants of metabotropic glutamate receptor subtype 5 in the rat brain and neuronal cells during development. *J Neurochem* **65**(4): 1536-1542.

Minakami R, Jinnai N and Sugiyama H (1997) Phosphorylation and calmodulin binding of the metabotropic glutamate receptor subtype 5 (mGluR5) are antagonistic in vitro. *J Biol Chem* **272**(32): 20291-20298.

Mockett BG, Guevremont D, Wutte M, Hulme SR, Williams JM and Abraham WC (2011) Calcium/calmodulin-dependent protein kinase II mediates group I metabotropic glutamate receptor-dependent protein synthesis and long-term depression in rat hippocampus. *J Neurosci* **31**(20): 7380-7391.

Mukherji S, Brickey DA and Soderling TR (1994) Mutational analysis of secondary structure in the autoinhibitory and autophosphorylation domains of calmodulin kinase II. *J Biol Chem* **269**(32): 20733-20738.

Niswender CM and Conn PJ (2010) Metabotropic glutamate receptors: physiology, pharmacology, and disease. *Annu Rev Pharmacol Toxicol* **50**: 295-322.

Noetzel MJ, Rook JM, Vinson PN, Cho HP, Days E, Zhou Y, Rodriguez AL, Lavreysen H, Stauffer SR, Niswender CM, Xiang Z, Daniels JS, Jones CK, Lindsley CW, Weaver CD and Conn PJ (2012) Functional impact of allosteric agonist activity of selective positive allosteric modulators of metabotropic glutamate receptor subtype 5 in regulating central nervous system function. *Mol Pharmacol* **81**(2): 120-133.

Oliet SH, Malenka RC and Nicoll RA (1997) Two distinct forms of long-term depression coexist in CA1 hippocampal pyramidal cells. *Neuron* **18**(6): 969-982.

Palmer MJ, Irving AJ, Seabrook GR, Jane DE and Collingridge GL (1997) The group I mGlu receptor agonist DHPG induces a novel form of LTD in the CA1 region of the hippocampus. *Neuropharmacology* **36**(11-12): 1517-1532.

Pasek JG, Wang X and Colbran RJ (2015) Differential CaMKII regulation by voltage-gated calcium channels in the striatum. *Mol Cell Neurosci* **68**: 234-243.

Raka F, Di Sebastiano AR, Kulhawy SC, Ribeiro FM, Godin CM, Caetano FA, Angers S and Ferguson SS (2015) Ca(2+)/calmodulin-dependent protein kinase II interacts with group I metabotropic glutamate and facilitates receptor endocytosis and ERK1/2 signaling: role of beta-amyloid. *Mol Brain* **8**: 21.

Rich RC and Schulman H (1998) Substrate-directed function of calmodulin in autophosphorylation of Ca2+/calmodulin-dependent protein kinase II. *J Biol Chem* **273**(43): 28424-28429.

Roche KW, Tu JC, Petralia RS, Xiao B, Wenthold RJ and Worley PF (1999) Homer 1b regulates the trafficking of group I metabotropic glutamate receptors. *J Biol Chem* **274**(36): 25953-25957.

Romano C, van den Pol AN and O'Malley KL (1996) Enhanced early developmental expression of the metabotropic glutamate receptor mGluR5 in rat brain: protein, mRNA splice variants, and regional distribution. *J Comp Neurol* **367**(3): 403-412.

Ronesi JA, Collins KA, Hays SA, Tsai NP, Guo W, Birnbaum SG, Hu JH, Worley PF, Gibson JR and Huber KM (2012) Disrupted Homer scaffolds mediate abnormal mGluR5 function in a mouse model of fragile X syndrome. *Nat Neurosci* **15**(3): 431-440, S431.

Saito H, Kimura M, Inanobe A, Ohe T and Kurachi Y (2002) An N-terminal sequence specific for a novel Homer1 isoform controls trafficking of group I metabotropic glutamate receptor in mammalian cells. *Biochem Biophys Res Commun* **296**(3): 523-529.

Schoepp DD, Jane DE and Monn JA (1999) Pharmacological agents acting at subtypes of metabotropic glutamate receptors. *Neuropharmacology* **38**(10): 1431-1476.

Shonesy BC, Jalan-Sakrikar N, Cavener VS and Colbran RJ (2014) CaMKII: a molecular substrate for synaptic plasticity and memory. *Prog Mol Biol Transl Sci* **122**: 61-87.

Silva AJ, Paylor R, Wehner JM and Tonegawa S (1992a) Impaired spatial learning in alpha-calcium-calmodulin kinase II mutant mice. *Science* **257**(5067): 206-211.

Silva AJ, Stevens CF, Tonegawa S and Wang Y (1992b) Deficient hippocampal long-term potentiation in alpha-calcium-calmodulin kinase II mutant mice. *Science* **257**(5067): 201-206.

Simonyi A, Schachtman TR and Christoffersen GR (2005) The role of metabotropic glutamate receptor 5 in learning and memory processes. *Drug News Perspect* **18**(6): 353-361.

Stephenson JR, Wang X, Perfitt TL, Parrish WP, Shonesy BC, Marks CR, Mortlock DP, Nakagawa T, Sutcliffe JS and Colbran RJ (2017) A Novel Human CAMK2A Mutation Disrupts Dendritic Morphology and Synaptic Transmission, and Causes ASD-Related Behaviors. *J Neurosci* **37**(8): 2216-2233.

Strack S, McNeill RB and Colbran RJ (2000) Mechanism and regulation of calcium/calmodulin-dependent protein kinase II targeting to the NR2B subunit of the N-methyl-D-aspartate receptor. *J Biol Chem* **275**(31): 23798-23806.

Uematsu K, Heiman M, Zelenina M, Padovan J, Chait BT, Aperia A, Nishi A and Greengard P (2015) Protein kinase A directly phosphorylates metabotropic glutamate receptor 5 to modulate its function. *J Neurochem* **132**(6): 677-686.

Valenti O, Conn PJ and Marino MJ (2002) Distinct physiological roles of the Gq-coupled metabotropic glutamate receptors Co-expressed in the same neuronal populations. *J Cell Physiol* **191**(2): 125-137.

Volk LJ, Daly CA and Huber KM (2006) Differential roles for group 1 mGluR subtypes in induction and expression of chemically induced hippocampal long-term depression. *J Neurophysiol* **95**(4): 2427-2438.

Wang X, Marks CR, Perfitt TL, Nakagawa T, Lee A, Jacobson DA and Colbran RJ (2017) A novel mechanism for Ca2+/calmodulin-dependent protein kinase II targeting to L-type Ca2+ channels that initiates long-range signaling to the nucleus. *J Biol Chem* **292**(42): 17324-17336.

Yang E and Schulman H (1999) Structural examination of autoregulation of multifunctional calcium/calmodulin-dependent protein kinase II. *J Biol Chem* **274**(37): 26199-26208.

Zhang S, Xie C, Wang Q and Liu Z (2014) Interactions of CaMKII with dopamine D2 receptors: roles in levodopa-induced dyskinesia in 6-hydroxydopamine lesioned Parkinson's rats. *Sci Rep* **4**: 6811.

Zhou Y, Takahashi E, Li W, Halt A, Wiltgen B, Ehninger D, Li GD, Hell JW, Kennedy MB and Silva AJ (2007) Interactions between the NR2B receptor and CaMKII modulate synaptic plasticity and spatial learning. *J Neurosci* **27**(50): 13843-13853.

Molecular Pharmacology Fast Forward. Published on October 3, 2018 as DOI: 10.1124/mol.118.113142
This article has not been copyedited and formatted. The final version may differ from this version.

Footnotes: This work was supported by grants from the National Institutes of Health [R01-MH063232] and [R01-NS078291] to R.J.C. [F31MH109196] to C.R.M. [T32-DK07563] to C.R.M., the American Heart Association [14PRE18420020] to X.W. and [15PRE25110020] to C.R.M. The content is solely the responsibility of the authors and does not necessarily represent the official views of the National Institutes of Health or other funding agencies. CRISPR/Cas9 pronuclear injections were performed by the Vanderbilt University School of Medicine Transgenic Mouse/ES Cell Shared Resource supported through the Cancer Center Support Grant [CA68485], the Vanderbilt Diabetes Research and Training Center [DK020593], and the Center for Stem Cell Biology.

Molecular Pharmacology Fast Forward. Published on October 3, 2018 as DOI: 10.1124/mol.118.113142
This article has not been copyedited and formatted. The final version may differ from this version.

Legends for Figures:

Figure 1. *Co-immunoprecipitation of mGlu$_5$ with mouse forebrain CaMKIIα*. Solubilized fractions from WT or CaMKIIα-KO mouse forebrain were immunoprecipitated using CaMKIIα-specific (α) or control (IgG) antibodies, as indicated. Inputs and immune complexes were analyzed by immunoblotting: mGlu5 was detected only in immune complexes isolated from WT tissue using the CaMKIIα antibody. Open and closed arrowheads indicate dimeric and monomeric species of mGlu$_5$. Representative of 3 similar experiments.

Figure 2. *CaMKII autophosphorylation at Thr286 enhances binding to the mGlu$_5$ C-terminal domain*. **A.** *Autophosphorylation of purified CaMKIIα*. Purified CaMKIIα was incubated with *Mg*$(C_2H_3O_2)_2$, $CaCl_2$, CaM, and ATP for either 90 s at 4°C or 10 min at 30°C and samples were immunoblotted for total or phospho-Thr286 CaMKII. While quantitative analysis (right) indicated that there was a similarly robust Thr286 autophosphorylation using these two conditions, the 10 min/30°C incubation resulted in a substantial reduction in electrophoretic mobility due to phosphorylation at additional unidentified sites. Data are plotted as the mean±SEM (n=3) and analyzed using a one-way ANOVA (p=0.0167, F=8.746, R square = 0.7446) with Sidak's *post-hoc* test for mulplicity adjusted *p* values: Control vs. 4°C, p=0.031. Control vs. 30°C, p=0.035. 4°C vs. 30°C, p=1.00 **B.** *The GST-mGlu$_{5a}$-CTD binds CaMKIIα following selective autophosphorylation at Thr286*. GST-mGlu$_{5a}$-CTD was incubated with purified CaMKIIα that had been preincubated as in panel A, and complexes were isolated using glutathione agarose. Immunoblot analyses revealed that CaMKIIα binding to the CTD was strongly enhanced by selective Thr286 autophosphorylation at 4°C, but that the autophosphorylation of additional sites on CaMKII at 30°C substantially reduced binding. Data are plotted as the mean±SEM (n=3) and

Molecular Pharmacology Fast Forward. Published on October 3, 2018 as DOI: 10.1124/mol.118.113142
This article has not been copyedited and formatted. The final version may differ from this version.

were analyzed using a one-way ANOVA (p=0.005, F=2.477, R square = 0.829) with Sidak's *post-hoc* test for multiplicity adjusted *p* values: Control vs. 4°C, p=0.009. 4°C vs. 30°C, p=0.011. Control vs. 30°C, p=1.00. **C.** *Binding of activated CaMKIIα to GST-mGlu$_{5a}$-CTD is disrupted by Ca^{2+}/CaM*. Purified CaMKIIα was autophosphorylated for 90 s at 4°C (see Panel A) and then incubated with GST-mGlu$_{5a}$-CTD in the absence or presence of excess Ca^{2+}/CaM (see Methods). Complexes were isolated using glutathione-agarose and then immunoblotted as indicated. Data are plotted as the mean±SEM; excess Ca^{2+}/CaM significantly reduced CaMKIIα binding ($p < 0.0001$ relative to theoretical value of 1.00 by one-sample t-test; n=4).

Figure 3. *Identification of CaMKII-binding determinants in the mGlu$_{5a}$-CTD*. **A.** *Alignment of part of the mGlu$_{5a}$-CTD with amino acid sequences surrounding known CaMKII-binding domains*. Tribasic residue motifs (highlighted) were identified within CaMKII-binding domains from other proteins, as well as within the CaMKII binding fragment in the CTD of mGlu$_{5a}$. Mutation of $R^{83}K^{84}R^{85}$ to AAA in the Ca$_V$1.3 N-terminal domain (NTD) disrupts the binding of CaMKII (Wang et al., 2017). The red and blue fonts indicate residues in each domain that are identical and homologous, respectively, with residues in the mGlu$_{5a}$ sequence. Underlined residues in the mGlu$_1$-CTD and the D_2 dopamine receptor (IL3: third intracellular loop) demark the sequences of synthetic peptides that were shown to compete for CaMKII binding (Jin et al., 2013a; Zhang et al., 2014). **B.** *Mutation of the tribasic residue motif in the mGlu$_{5a}$ CTD disrupts CaMKII binding*. Thr286 autophosphorylated CaMKIIα (90 s/4°C protocol) was incubated with GST-mGlu$_{5a}$-CTD (WT or with a $K^{866}R^{867}R^{868}$ to AAA mutation) and complexes were analyzed as in Fig. 1. The $K^{866}R^{867}R^{868}$/AAA mutation essentially abolishes CaMKII binding Data are plotted as the mean±SEM ($p = 0.003$ by a one sample t-test; n=4).

Molecular Pharmacology Fast Forward. Published on October 3, 2018 as DOI: 10.1124/mol.118.113142
This article has not been copyedited and formatted. The final version may differ from this version.

Figure 4. *Role of the CTD in full-length $mGlu_{5a}$ binding to activated CaMKIIα*. **A.** *CaMKII activation enhances interaction with full length $mGlu_5$.* Solubilized fractions of HEK293A cells expressing HA-tagged $mGlu_{5a}$ and/or mApple-tagged WT CaMKIIα (as indicated above lanes) were pre-incubated with Ca^{2+}/CaM, $MgAc_2$, and ATP in the presence or absence of excess EDTA (–/+ activation, respectively) and then immunoprecipitated using antibodies to the HA epitope. Lysates and immune complexes were analyzed by immunoblotting, as indicated. CaMKIIα activation results in robust Thr-286 autophosphorylation, which increases CaMKIIα association with HA-$mGlu_{5a}$ Data are plotted as the mean±SEM (p=0.043; one-sample t-test; n=4). Open and closed arrowheads indicate dimeric and monomeric species of $mGlu_{5a}$. **B.** *CaMKII association with full-length $mGlu_{5a}$ is disrupted by mutation of the CTD tribasic residue motif*. Solubilized fractions of HEK293A cells expressing HA-$mGlu_5$ (WT or with the $K^{866}R^{867}R^{868}$/AAA mutation) and mApple-tagged CA-CaMKIIα were immunoprecipitated using antibodies to the HA epitope. Lysates and the immune complexes were analyzed by immunoblotting, as indicated. The $K^{866}R^{867}R^{868}$/AAA mutation reduced the association of CA-CaMKIIα with HA-$mGlu_5$ Data are plotted as the mean±SEM (p=0.028; one sample t-test; n=4).

Figure 5. *CaMKII enhances the cell-surface expression of $mGlu_{5a}$ via interaction with the CTD*. Cell surface biotinylation analyses of HEK293A cells expressing $mGlu_{5a}$ (WT or with $K^{866}R^{867}R^{868}$/AAA mutation in the CTD) with either mApple or mApple-tagged CA-CaMKIIα. The co-expression of CA-CaMKIIα increased steady-state surface expression levels of WT $mGlu_{5a}$ (p=0.036; one sample t-test; n=6), but not of the $K^{866}R^{867}R^{868}$/AAA mutant Data are plotted as the mean±SEM (p = 0.569; one sample t-test; n=5).

Molecular Pharmacology Fast Forward. Published on October 3, 2018 as DOI: 10.1124/mol.118.113142
This article has not been copyedited and formatted. The final version may differ from this version.

Figure 6. *CaMKIIα regulates $mGlu_{5a}$-stimulated Ca^{2+} mobilization in 293A-$5a^{LOW}$ cells*. Time courses of intracellular Ca^{2+} responses to glutamate were measured by changes in Fluo-4 fluorescence in stable 293A-$5a^{LOW}$ cells in 96 well plates. **A.** *Time courses of Ca^{2+} responses*. Example of calcium responses to increasing glutamate concentrations collected in a row of 8-wells. **B.** Overlay of individual Ca^{2+} responses to increasing concentrations of glutamate (labeled by colors in Panel A) from 293A-$5a^{LOW}$ cells transiently transfected to express mApple control, mApple-CaMKIIα-WT or mApple-CA-CaMKIIα from a representative experiment. **C.** *Concentration response curves*. Initial peak Ca^{2+} responses (ΔF/F0) at each concentration were normalized to the maximal glutamate-stimulated response in control (mApple-transfected) cells within each experiment. Normalized Ca^{2+} responses are plotted as the mean±SEM (n=5 experiments) as a function of glutamate concentration. The expression of CaMKIIα-WT had no impact on the Ca^{2+} response curve but the expression of CA-CaMKIIα reduced peak Ca^{2+} responses (multiple comparisons two-way ANOVA: Sources of Variation: CaMKII $p<0.0001$, Interaction $p=0.029$. Tukey's *post hoc* test for multiplicity adjusted *p* values: mApple vs. WT, $p = 0.926$, mApple vs. CA-CaMKIIα, $p <0.0001$. WT vs. CA-CaMKIIα, $p=0.0002$). The inset table shows the maximum response (Max), EC_{50} (μM), and Hill coefficient (±SEM) obtained by fitting the data in GraphPad Prism.

Figure 7. *CaMKIIα binding to the CTD is required for modulation $mGlu_{5a}$-stimulated Ca^{2+} mobilization*. HEK293A cells were transiently transfected to express $mGlu_{5a}$ (WT or $K^{866}RR^{868}$/AAA) with either mApple or mApple-CA-CaMKIIα for single-cell Fura-2 Ca^{2+}

Molecular Pharmacology Fast Forward. Published on October 3, 2018 as DOI: 10.1124/mol.118.113142
This article has not been copyedited and formatted. The final version may differ from this version.

imaging (see Methods). **A, D.** *Representative data from a single experiment*. Averaged normalized changes in fluorescence from 58-114 cells (ΔF/F0: mean±SEM) expressing $mGlu_{5a}$-WT (**A**) or $mGlu_5$-$K^{866}R^{867}R^{868}$/AAA (**D**) in the presence (blue lines) or absence (red lines) of mApple-CA-CaMKIIα. The inset graphs show line-fits for time courses of the decline of Ca^{2+} signals from the peak ΔF/F0 under each condition. **B, C, E, F.** *Summary data*. The bar graphs depict mean±SEM values for peak Ca^{2+} signals (ΔF/F0) (**B, E**) and half-lives for the decline in Ca^{2+} signals (**C, F**) with super-imposed data points from each experiment (n=5). Expression of constitutively-active mApple-CA-CaMKII decreases the peak Ca^{2+} signal but increases the half-life of the Ca^{2+} signal with $mGlu_{5a}$-WT (B, p=0.009. C, p=0.001), but has no significant effect on the $mGlu_{5a}$-$K^{866}R^{867}R^{868}$/AAA mutant that disrupts CaMKII binding to the CTD (E, p=0.155. F, p=0.415). Paired Student's t-tests were used for statistical comparisons in each panel.

Molecular Pharmacology Fast Forward. Published on October 3, 2018 as DOI: 10.1124/mol.118.113142
This article has not been copyedited and formatted. The final version may differ from this version.

Figure 1

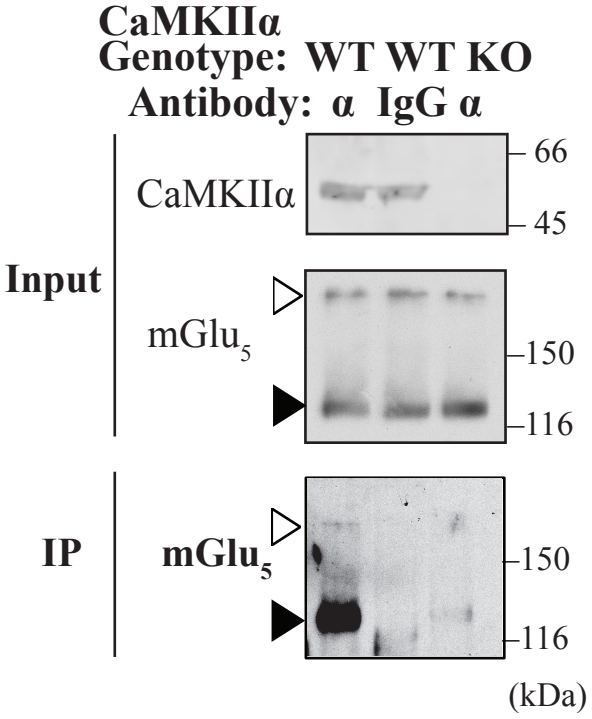

Molecular Pharmacology Fast Forward. Published on October 3, 2018 as DOI: 10.1124/mol.118.113142
This article has not been copyedited and formatted. The final version may differ from this version.

Figure 2

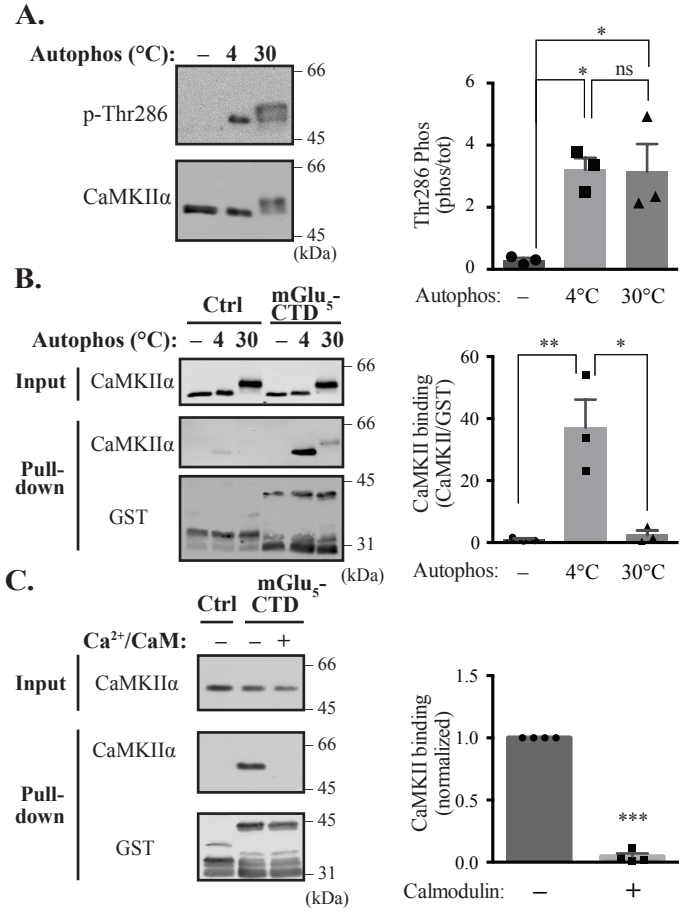

Molecular Pharmacology Fast Forward. Published on October 3, 2018 as DOI: 10.1124/mol.118.113142
This article has not been copyedited and formatted. The final version may differ from this version.

Figure 3

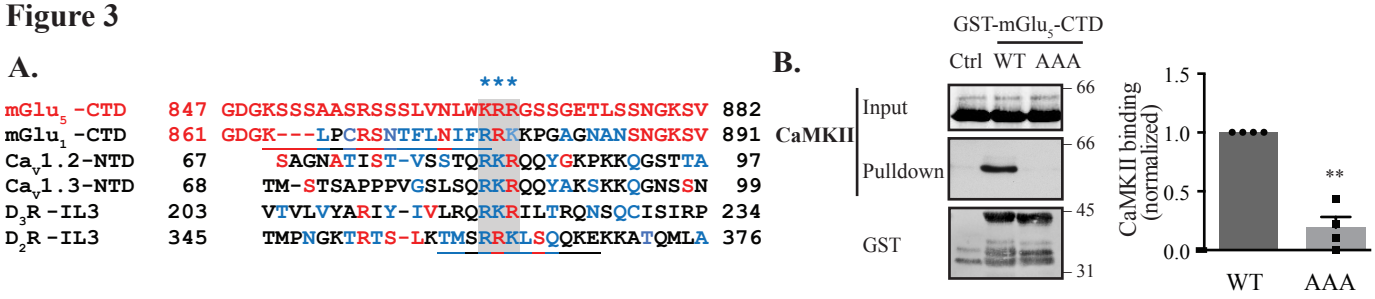

Molecular Pharmacology Fast Forward. Published on October 3, 2018 as DOI: 10.1124/mol.118.113142
This article has not been copyedited and formatted. The final version may differ from this version.

Figure 4

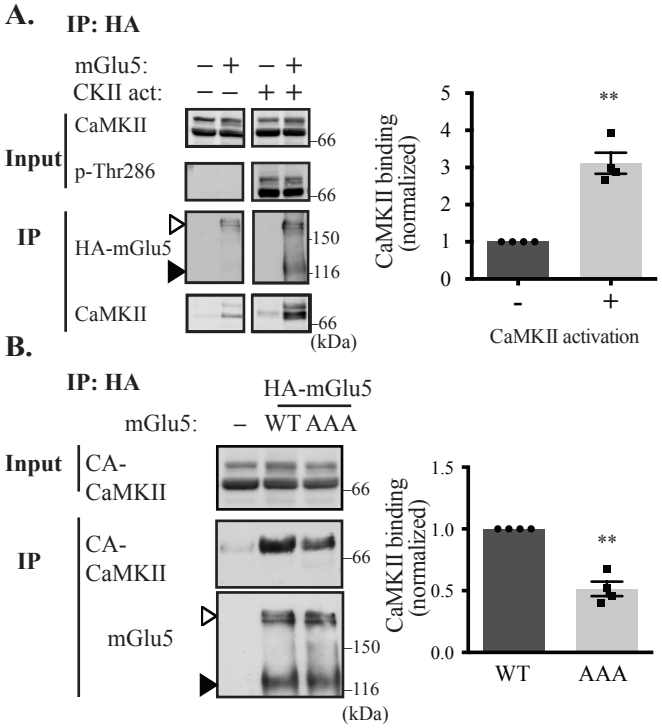

Molecular Pharmacology Fast Forward. Published on October 3, 2018 as DOI: 10.1124/mol.118.113142
This article has not been copyedited and formatted. The final version may differ from this version.

Figure 5

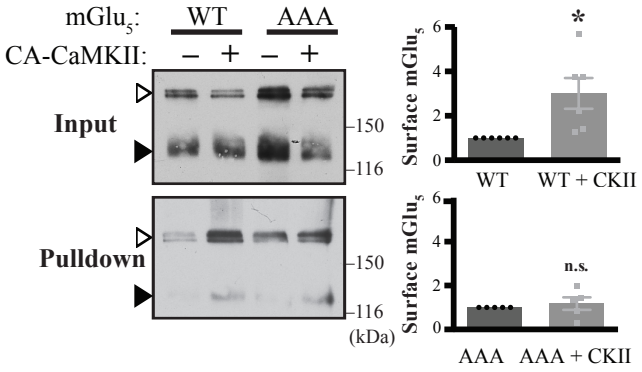

Molecular Pharmacology Fast Forward. Published on October 3, 2018 as DOI: 10.1124/mol.118.113142
This article has not been copyedited and formatted. The final version may differ from this version.

Figure 6

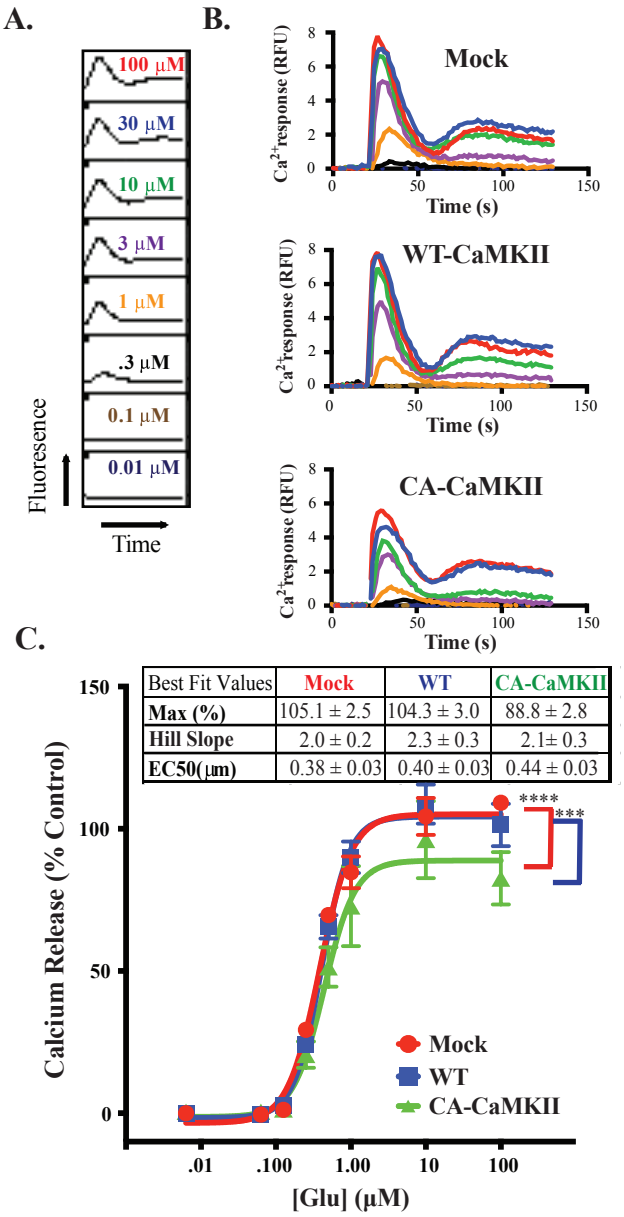

Molecular Pharmacology Fast Forward. Published on October 3, 2018 as DOI: 10.1124/mol.118.113142
This article has not been copyedited and formatted. The final version may differ from this version.

Figure 7